Hindawi
Journal of Chemistry
Volume 2020, Article ID 2036585, 10 pages
https://doi.org/10.1155/2020/2036585

*Research Article*

# Using Topomer Comparative Molecular Field Analysis to Elucidate Activity Differences of Aminomethylenethiophene Derivatives as Lysyl Oxidase Inhibitors: Implications for Rational Design of Antimetastatic Agents for Cancer Therapy

**Jing Han,[1] Guochao Yan,[2] Jianping Feng,[2] Xianglin Yang,[3] and Yuan Zhou[4]**

[1]*Department of Electronic and Information Engineering, Changsha Social Work College, Changsha 410004, Hunan, China*
[2]*College of Mining Engineering, Taiyuan University of Technology, Taiyuan, Shanxi, China*
[3]*Western Australia School of Mines: Minerals, Energy and Chemical Engineering, Curtin University, Kalgoorlie, WA 6430, Australia*
[4]*College of Chemistry and Chemical Engineering, Hunan Institute of Engineering, Xiangtan 411104, Hunan, China*

Correspondence should be addressed to Guochao Yan; ygchao2000@126.com and Xianglin Yang; xianglin.yang@curtin.edu.au

Received 1 December 2019; Accepted 2 April 2020; Published 16 May 2020

Academic Editor: Gabriel Navarrete-Vazquez



Topomer comparative molecular field analysis (topomer CoMFA) is applied to the quantitative structure-activity relationship (QSAR) study of aminomethylenethiophene (AMT) derivatives as lysyl oxidase (LOX) inhibitors. A total of thirty-six AMT derivatives were selected to build the QSAR model. The established topomer CoMFA model has the non-cross-validated correlation coefficient ($r^2$) of 0.912 and the leave-one-out correlation coefficient ($q^2$) of 0.540, which is statistically significant. The theoretically predicted anti-LOX potency agrees well with the experimentally observed inhibitory activity, proving the reasonable predictive ability of the QSAR model. The effect of molecular field information on the LOX inhibition of substituted aminomethylenethiophene was discussed in detail. The structural modification of the aminomethylenethiophene scaffold was carried out, and novel AMT derivatives with theoretically decent LOX inhibition were proposed. The topomer CoMFA modeling could provide a quantitative perspective into the structure-activity relationship of AMT derivatives and potentially speed up the rational design of LOX inhibitors as antimetastatic agents for cancer therapy.

## 1. Introduction

Lysyl oxidase and its family members (i.e., LOXL1–4) are amine oxidases that chemically cross-link elastin and collagens in the tumor extracellular matrix [1–3]. LOX originally exists as a catalytically inactive proprotein, which is converted to an active enzyme by proteases. LOX and LOXL1–4 share a common catalytic domain that incorporates a lysine tyrosylquinone cofactor, where oxidative deamination reaction that turns peptidyl lysine residues ($H_2NCH_2R$) into $\alpha$-aminoadipic-$\delta$-semialdehyde (O=CHR) occurs [1]. The resulting aldehyde residues chemically cross-link with neighbouring nucleophilic functionalities, yielding insoluble extracellular protein matrices.

LOX and LOXL2 play important roles in stimulating tumor growth in various kinds of cancer [4–6]. Noticeably, LOX has been proved to be a significant mediator of cancer metastasis [7]. Thus, therapeutic agents inhibiting the activity of LOX are suggested as cancer treatments, particularly against metastasis where successful therapeutic methods are currently rare.

To date, few drug-like inhibitors of LOX have been reported [8, 9]. It was published that trifluoromethyl-substituted aminomethylene-pyridine exhibited weak inhibition against LOX [8]. Until recently, aminomethylenethiophene (AMT) derivatives were proved to be potent inhibitors of LOX and, more importantly, can significantly reduce tumor growth as well as metastatic burden in a mouse model [9, 10].

Table 1: Molecular structures, experimentally recorded, and theoretically predicted anti-LOX potency of the substituted amino-methylenethiophene.

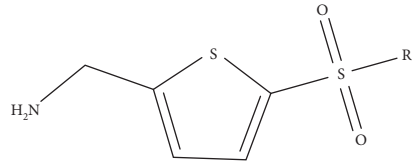


| Number | R | LOX –log ($IC_{50}$) | |
|---|---|---|---|
| | | Experimental | Predicted |
| $1^t$ | 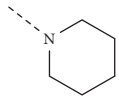 | −1.2788 | −0.78 |
| 2 |  | −1.8513 | −1.5 |
| 3 | 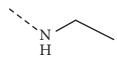 | −1.4624 | −1.3 |
| 4 | 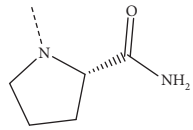 | −1.0792 | −1.14 |
| 5 | 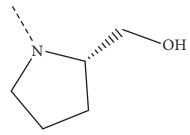 | −0.5052 | −0.66 |
| 6 | 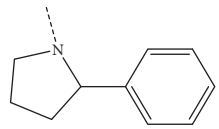 | −0.5798 | −0.64 |
| 7 | 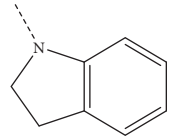 | −0.2788 | −0.25 |
| $8^t$ | 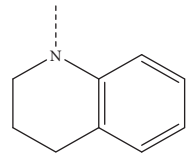 | −0.4150 | −0.21 |
| 9 | 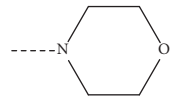 | −1.3522 | −1.49 |
| 10 | 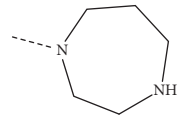 | −1.0434 | −0.84 |
| $11^t$ | 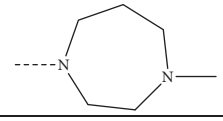 | −0.4914 | −0.46 |

Table 1: Continued.

| Number | R | LOX −log ($IC_{50}$) Experimental | Predicted |
|---|---|---|---|
| 12 | 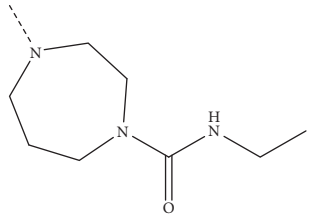 | −0.3222 | −0.09 |
| 13 | 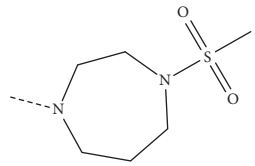 | 0.0315 | −0.02 |
| 14 | 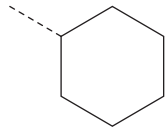 | −0.3222 | −0.63 |
| 15 | 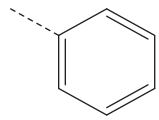 | −0.2305 | −0.21 |
| 16 | 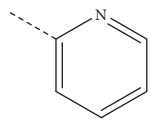 | −0.3617 | −0.37 |
| 17 | 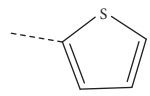 | −0.0394 | −0.41 |
| 18[t] | 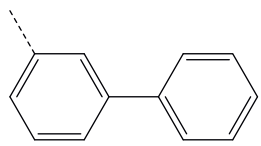 | −0.8062 | −0.12 |
| 19 | 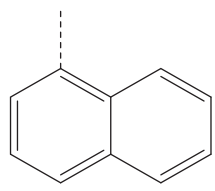 | −0.6721 | −0.33 |
| 20 | 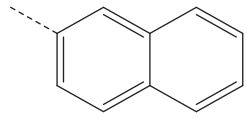 | 0.1612 | 0.21 |
| 21 | 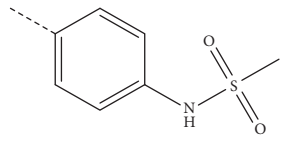 | −0.4472 | −0.64 |
| 22 | 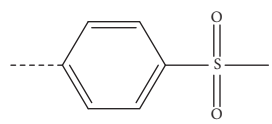 | 0.5850 | 0.39 |

Table 1: Continued.

| Number | R | LOX $-\log(IC_{50})$ Experimental | Predicted |
|---|---|---|---|
| 23 | 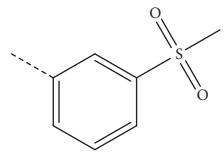 | 0.4089 | 0.67 |
| 24[t] | 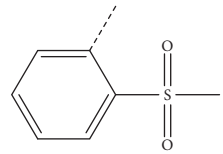 | −0.1461 | −0.19 |
| 25 | 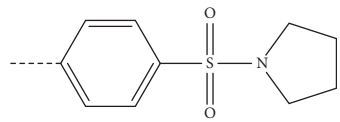 | 0.0362 | 0.04 |
| 26[t] | 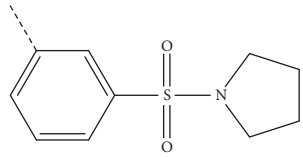 | 0.2147 | 0.15 |
| 27 | 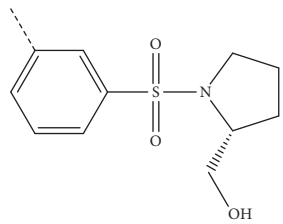 | 0.3768 | 0.52 |
| 28[t] | 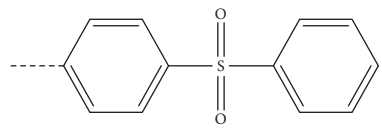 | −0.2553 | 0.28 |
| 29 | 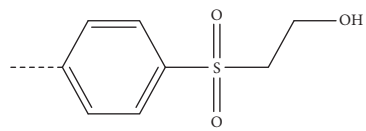 | 0.5376 | 0.50 |
| 30 | 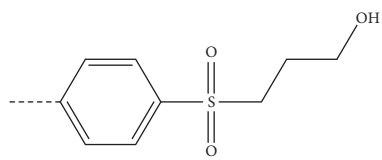 | 0.3468 | 0.23 |
| 31 | 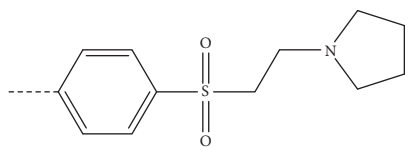 | 0.2291 | 0.28 |

Table 1: Continued.

| Number | R | LOX −log ($IC_{50}$) Experimental | Predicted |
|---|---|---|---|
| 32 | 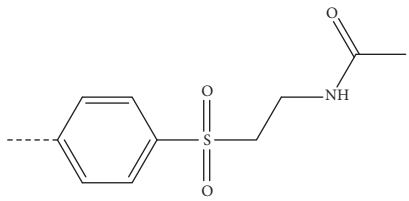 | 0.1427 | 0.05 |
| 33[t] | 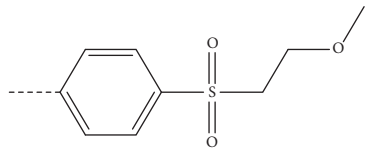 | −0.2305 | 0.39 |
| 34 | 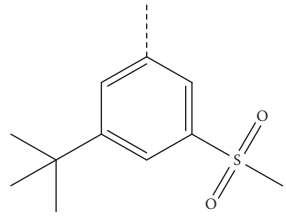 | −0.0792 | 0.03 |
| 35 | 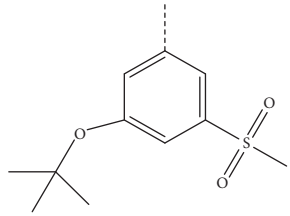 | −0.2788 | −0.14 |
| 36[t] | 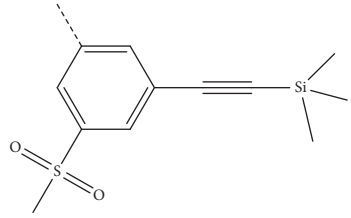 | −0.3979 | −0.34 |
| 37 | 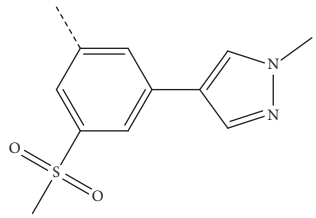 | −0.2305 | −0.26 |
| 38 | 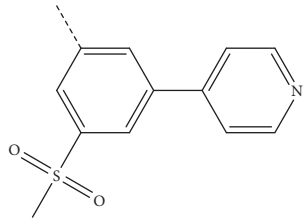 | −0.1903 | −0.12 |

Table 1: Continued.

| Number | R | LOX $-\log (IC_{50})$ | |
|---|---|---|---|
| | | Experimental | Predicted |
| 39 | 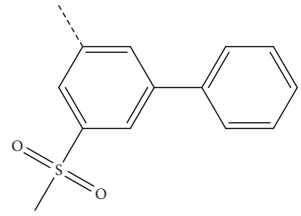 | 0.0458 | −0.16 |
| 40 | 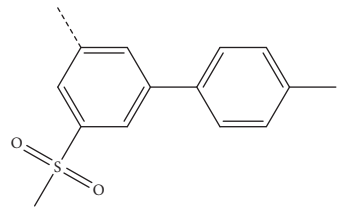 | −0.0414 | −0.24 |
| 41 | 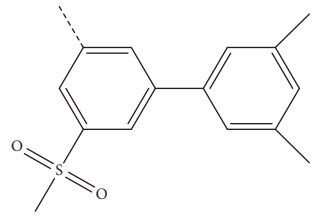 | −0.5682 | −0.50 |
| 42[t] | 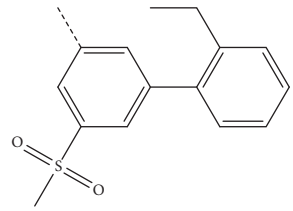 | −0.8129 | −0.07 |
| 43 | 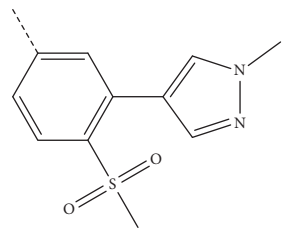 | 0.1337 | 0.09 |
| 44 | 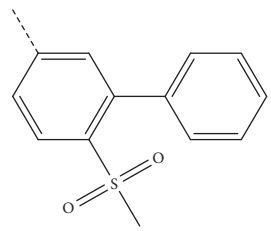 | 0.0942 | 0.17 |
| 45 | 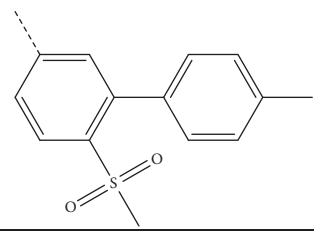 | 0.0915 | 0.13 |

[t]Test set compound.

The preliminary structure-activity relationship study of AMT derivatives has been performed, which was dictated by chemical intuition and serendipity [9, 11–13]. Considering the fact that we are entering the era of big data and artificial intelligence, empirical and labor-intensive approaches are being incrementally replaced by automatic and rational strategies [14–17]. Consistent with this emerging trend, sophisticated drug design method (i.e., topomer CoMFA) in this paper is introduced into the three-dimensional quantitative structure-activity relationship (3D-QSAR) study of aminomethylenethiophene derivatives, which holds great promise for rational design of LOX inhibitors with improved potency.

## 2. Materials and Methods

*2.1. Substituted Aminomethylenethiophene.* The aminomethylenethiophene (AMT) derivatives and their anti-LOX potency are taken from the recently published literature [9]. The LOX inhibition values of AMT derivatives, that is, LOX $IC_{50}$ ($\mu$M), were obtained under identical experimental conditions [9]. The molecular structures of AMT derivatives and their anti-LOX potency are shown in Table 1. Thirty-six of the forty-five aminomethylenethiophene-based inhibitors were chosen as the training set, while the remaining nine molecules were used as the test set. During the selection of the training and test set, great efforts were made to ensure that the most potent, moderately active, and low active AMT inhibitors were included in the training set to spread the activity range. The test set compounds were selected in such a manner that at least one structural analog of the training set was chosen for the test set. Each AMT derivative was geometrically optimized by the Tripos force field under the convergence criterion of 0.005 kcal/mol [15, 16]. The MMFF94 method was utilized to determine the partial atomic charges of AMT derivatives [15, 18].

*2.2. Topomer CoMFA.* The molecular modelling of 3D-QSAR was carried out using SYBYL 8.1.1 software running on a HP Z600 workstation. For the topomer CoMFA method, the aim is to build a quantitative relationship between molecular field information of topomers (i.e., steric and electrostatic fields) and LOX inhibition activity [19–21]. A topomer indicates an invariant three-dimensional representation of the molecular fragment with absolute orientation and conformation [21]. It is well known that comparative molecular field analysis (CoMFA) is very sensitive to the molecular alignment scheme by which the training set compounds are superimposed over the maximum common substructure [22]. To circumvent this problem, topomer CoMFA is invented as an alignment-free 3D-QSAR technique [19, 20].

In this paper, topomer comparative molecular filed analysis (topomer CoMFA) is used to build the quantitative relationship between the molecular field information and the anti-LOX potency of aminomethylenethiophene derivatives.

*2.3. Statistical Evaluation of the QSAR Model.* To avoid overfitted 3D-QSAR model, partial least squares (PLS) is utilized to correlate the molecular filed descriptors with the anti-LOX potency of AMT derivatives [23].

The predictive capability of the QSAR model is measured by the cross-validated coefficient ($q^2$), which is determined by the leave-one-out cross-validation procedure and can be formulated as

$$q^2 = 1 - \frac{\sum\left(Y_{\text{pred}} - Y_{\text{actual}}\right)^2}{\sum\left(Y_{\text{actual}} - Y_{\text{mean}}\right)^2}, \quad (1)$$

where $Y_{\text{pred}}$, $Y_{\text{actual}}$, and $Y_{\text{mean}}$ are the theoretically predicted, experimentally measured, and mean LOX inhibition activities of the training set, respectively.

## 3. Results and Discussion

*3.1. Molecular Fragmentation.* The structural variation of AMT derivatives lies in the R substitute, while aminomethylenethiophene is the common scaffold. Thus, all the substituted aminomethylenethiophenes are fragmented into two parts: (1) the common scaffold and (2) R substituent. The fragmentation pattern is shown in Figure 1.

*3.2. Statistical Analysis of the QSAR Model.* The statistical results of the topomer CoMFA model are presented in Table 2, which shows the non-cross-validation correlation coefficient ($r^2$) of 0.912 and cross-validation correlation coefficient ($q^2$) of 0.540. It is recognized that a 3D-QSAR model would have decent predictive ability provided that $q^2$ is greater than 0.5 and $r^2$ is more than 0.6 [19, 24, 25]. As such, the resultant 3D-QSAR model in this paper should be statistically robust. In terms of the topomer CoMFA model, the predicted anti-LOX potency of the AMT derivatives is listed in Table 1. The experimentally measured LOX inhibition activities versus the theoretically predicted values are graphically shown in Figure 2, and the data points reside closely to the diagonal line. It is known that if the leave-one-out correlation coefficient of a 3D-QSAR model is above 0.3, the likelihood of chance correlation could be less than 5% [26]. Furthermore, the correlation coefficient ($R^2$) for the test set is 0.6637, which indicates a decent predictive power of the otpomer 3D-QSAR model. Therefore, the built topomer CoMFA model in our paper should be statistically significant and has sound predictive ability, which could be used to predict and screen the untested AMT derivatives [19, 20, 25, 27].

*3.3. Topomer CoMFA Contour Analysis.* Given that the R substitute is the main factor governing the anti-LOX potency of AMT derivatives, the molecular field contour map of the R2 fragment is presented in Figure 3. Compound 22 with the highest LOX inhibition was employed as the reference molecule. Actually, Figure 3 provides hints about the possible regions for the structural modification of R2 fragments (i.e., the blue area favors the electron-donating substituent and the green area for steric groups, while the red area is

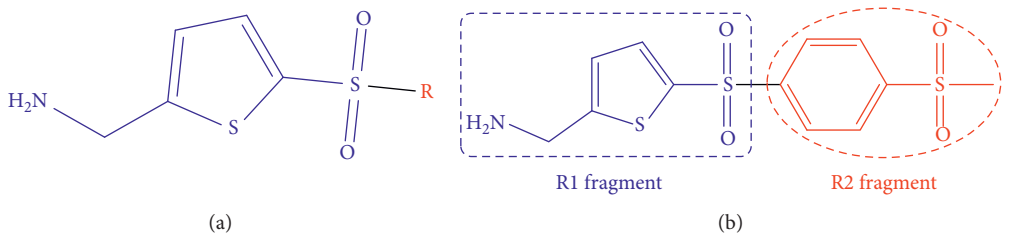


Figure 1: (a) Molecular structure of the aminomethylenethiophene derivatives. (b) The splitting mode for the topomer CoMFA modelling (using compound 22 as the reference).

Table 2: Statistical results of the topomer CoMFA model.

| Statistical parameters | |
|---|---|
| $F$ values | 62.193 |
| ONC | 5 |
| SEE | 0.180 |
| $r^2$ | 0.912 |
| $q^2$ | 0.540 |

$F$: significant test value. ONC: optimal number of components (LVs). SEE: standard error of estimate. $r^2$: non-cross-validation correlation coefficient. $q^2$: leave-one-out cross-validation correlation coefficient.

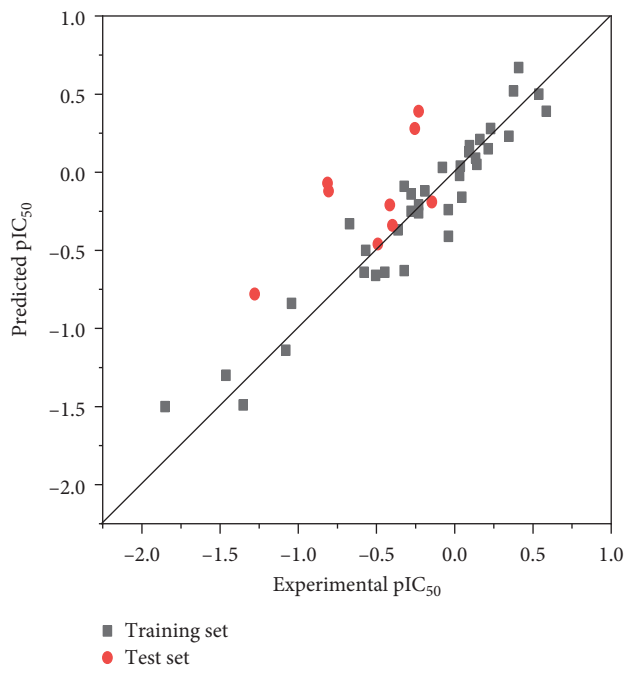


Figure 2: Experimental versus predicted anti-LOX potency. The training and the test set are displayed in squared (black) and circled (red) points, respectively.

favourable for electron-withdrawing substituent and the yellow area for the less steric groups).

The steric contour map of the R2 fragment is shown in Figure 3(a). In Figure 3(a), large polyhedra covering the 4-position of phenyl signify that steric hindrance at this location may be beneficial for improving the anti-LOX potency of AMT derivatives, which is convincingly confirmed by comparing the LOX inhibition activity of compound 15 with compound 22. Due to the sole introduction of methanesulfonyl into the 4-position of phenyl, the anti-LOX potency of compound 22 ($IC_{50}$: 0.26) is significantly improved as compared to compound 15 ($IC_{50}$: 1.7). The yellow polyhedra revolving around the 3-position of phenyl indicate that sterically bulky groups at this location may exert negative impact on the LOX inhibition of AMT derivatives, which is unambiguously validated by the comparison of compound 15 and compound 18; the LOX inhibition activity of the latter molecule ($IC_{50}$: 6.4) is much lower than the former compound ($IC_{50}$: 1.7) because of the addition of benzene at the 3-position of phenyl.

The electrostatic contour plots of the R2 fragment are displayed in Figure 3(b). In Figure 3(b), a red contour encapsulating the end of methanesulfonyl moiety implies that electron-donating groups at this end disfavor the LOX inhibition, which is clearly verified through comparing the structures and anti-LOX potency of compound 28 ($IC_{50}$: 1.8) and compounds 29–32 ($IC_{50}$: 0.29~0.72); compound 28 has a benzene substituent (i.e., electron-donating group) at the end of methanesulfonyl moiety, while compounds 29–32 have oxygen or nitrogen-containing groups (i.e., electron-withdrawing groups).

## 4. Newly Designed Compound and Predicted Anti-LOX Potency

Since the above 3D-QSAR model is statistically significant, it would be of utmost importance to theoretically design new molecule with enhanced LOX inhibition. The scaffold of aminomethylenethiophene was modified by various substituents, and the anti-LOX potency of the resulting AMT derivatives was predicted in terms of the already established 3D-QSAR model. Two of the newly designed AMT derivatives with the theoretically decent LOX inhibition are presented in Table 3. Though the theoretically predicted anti-LOX potency of the two novel compounds is slightly lower as compared to compound 22, it should be noted that

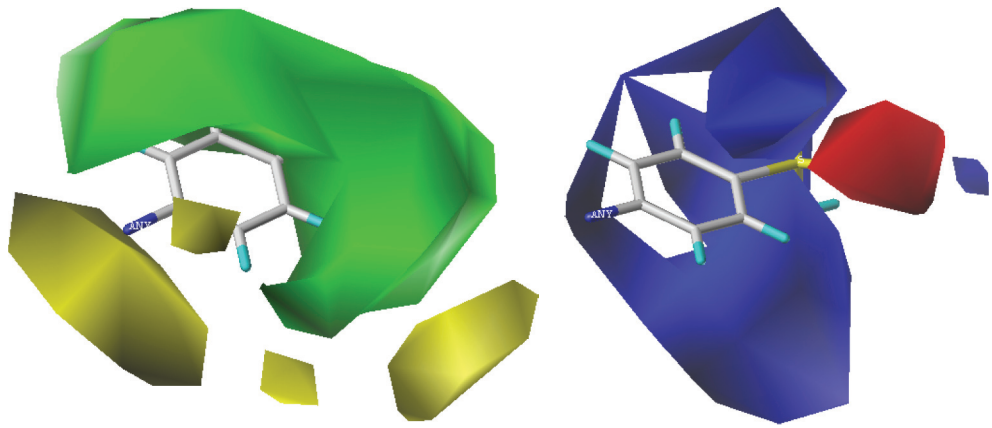

(a) (b)

Figure 3: Molecular field contour map pertaining to the R2 fragments using compound 22 as the reference. (a) Steric contours of the R2 fragment. (b) Electrostatic contours of the R2 fragment. Yellow contours imply that less steric hindrance is favourable, while green polyhedra indicate that the sterically bulky group is beneficial. Blue contours signify that the electron-donating groups are favored, while red contours reveal that the electron-withdrawing substituents are preferred.

Table 3: Newly designed molecules and predicted anti-LOX potency.

| Novel compounds | Predicted $pIC_{50}$ |
|---|---|
| 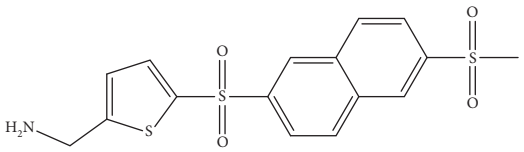 | 0.48 |
| 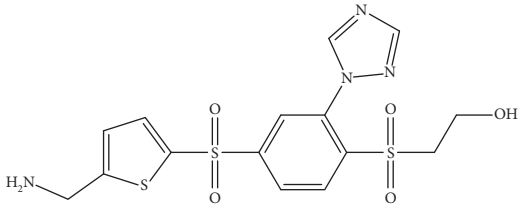 | 0.32 |

great caution is necessary in using QSAR to make predictions that extrapolate beyond the area of knowledge of the training set [28, 29]. In addition, these two newly proposed AMT derivatives should be synthetised to experimentally determine their LOX inhibition activity.

## 5. Conclusion

In this work, the topomer CoMFA method is applied to the quantitative structure-activity relationship study of aminomethylenethiophene (AMT) derivatives as novel lysyl oxidase (LOX) inhibitors. The resulting topomer CoMFA model is effective for estimating anti-LOX potency of the AMT derivatives. Molecular field information has illustrated the critical structural factors governing the LOX inhibition activity of substituted aminomethylenethiophene. In terms of the developed topomer CoMFA model, the theoretically predicted anti-LOX potency of AMT derivatives matched well with the experimentally measured values, indicating the reasonable predictive ability of the QSAR model. The newly designed AMT derivatives with theoretically decent anti-LOX potency have been proposed. This study may serve as the stepping stone for the rational design/selection of LOX inhibitors as antimetastatic agents for cancer therapy.

## Data Availability

All the data used to support the findings of this study are included within the article.

## Conflicts of Interest

The authors declare no conflicts of interest.

## Acknowledgments

This work was financially supported by the National Natural Science Foundation of China (Grant no. 51974195). Professor Yuan Zhou was greatly acknowledged for the fruitful discussion.

## Supplementary Materials

3D-QSAR (i.e., topomer CoMFA) was utilized to rationalize the activity differences of aminomethylenethiophene derivatives as lysyl oxidase (LOX) inhibitors, resulting in newly designed compounds with decent LOX inhibition potency. (*Supplementary Materials*)

## References

[1] H. A. Lucero and H. M. Kagan, "Lysyl oxidase: an oxidative enzyme and effector of cell function," *Cellular and Molecular Life Sciences CMLS*, vol. 63, no. 19-20, pp. 2304–2316, 2006.

[2] H. M. Kagan and F. Ryvkin, "Lysyl oxidase and lysyl oxidase-like enzymes," in *The Extracellular Matrix: An Overview*,

R. P. Mecham, Ed., pp. 303–335, Springer, Berlin, Germany, 1st edition, 2011.

[3] J. Finney, H.-J. Moon, T. Ronnebaum, M. Lantz, and M. Mure, "Human copper-dependent amine oxidases," *Archives of Biochemistry and Biophysics*, vol. 546, pp. 19–32, 2014.

[4] H. E. Barker, T. R. Cox, and J. T. Erler, "The rationale for targeting the LOX family in cancer," *Nature Reviews Cancer*, vol. 12, no. 8, pp. 540–552, 2012.

[5] T. R. Cox, A. Gartland, and J. T. Erler, "Lysyl oxidase, a targetable secreted molecule involved in cancer metastasis," *Cancer Research*, vol. 76, no. 2, pp. 188–192, 2016.

[6] K. A. Johnston and K. M. Lopez, "Lysyl oxidase in cancer inhibition and metastasis," *Cancer Letters*, vol. 417, pp. 174–181, 2018.

[7] J. T. Erler, K. L. Bennewith, M. Nicolau et al., "Lysyl oxidase is essential for hypoxia-induced metastasis," *Nature*, vol. 440, no. 7088, pp. 1222–1226, 2006.

[8] J. H. Hutchinson, M. W. Rowbottom, D. Lonergan et al., "Small molecule lysyl oxidase-like 2 (LOXL2) inhibitors: the identification of an inhibitor selective for LOXL2 over LOX," *ACS Medicinal Chemistry Letters*, vol. 8, no. 4, pp. 423–427, 2017.

[9] L. Leung, D. Niculescu-Duvaz, D. Smithen et al., "Anti-metastatic inhibitors of lysyl oxidase (LOX): design and structure-activity relationships," *Journal of Medicinal Chemistry*, vol. 62, no. 12, pp. 5863–5884, 2019.

[10] H. R. Tang, L. Leung, G. Saturno et al., "Lysyl oxidase drives tumour progression by trapping EGF receptors at the cell surface," *Nature Communications*, vol. 8, p. 14909, 2017.

[11] R. L. Sawant, P. D. Lanke, and J. B. Wadekar, "Tyrosinase inhibitory activity, 3D QSAR, and molecular docking study of 2,5-disubstituted-1,3,4-oxadiazoles," *Journal of Chemistry*, vol. 2013, Article ID 849782, 7 pages, 2013.

[12] K. T. Butler, D. W. Davies, H. Cartwright, O. Isayev, and A. Walsh, "Machine learning for molecular and materials science," *Nature*, vol. 559, no. 7715, pp. 547–555, 2018.

[13] O. Trelles, P. Prins, M. Snir, and R. C. Jansen, "Big data, but are we ready?" *Nature Reviews Genetics*, vol. 12, no. 3, p. 224, 2011.

[14] K. S. Bhadoriya, S. V. Jain, S. B. Bari, M. L. Chavhan, and K. R. Vispute, "3D-QSAR study of indol-2-yl ethanones derivatives as novel indoleamine 2,3-dioxygenase (IDO) inhibitors," *E-Journal of Chemistry*, vol. 9, no. 4, pp. 1753–1759, 2012.

[15] G. Yan, X. Yang, B. Albijanic, Y. Zhou, Y. Zhou, and X. Zhu, "A new tool to rationally design highly efficient organic sensitizers for dye-sensitized solar cells: a three-dimensional quantitative structure-activity relationship (3D-QSAR) perspective," *Solar Energy*, vol. 184, pp. 187–194, 2019.

[16] X. Yang, B. Albijanic, Y. Zhou, Y. Zhou, and X. Zhu, "Using 3D-QSAR to predict the separation efficiencies of flotation collectors: implications for rational design of non-polar side chains," *Minerals Engineering*, vol. 129, pp. 112–119, 2018.

[17] F. M. Abu-Awwad, "QSAR study of the biologically active organosulfurs in natural products," *E-Journal of Chemistry*, vol. 7, no. S1, pp. S335–S343, 2010.

[18] K.-C. Tsai, Y.-C. Chen, N.-W. Hsiao et al., "A comparison of different electrostatic potentials on prediction accuracy in CoMFA and CoMSIA studies," *European Journal of Medicinal Chemistry*, vol. 45, no. 4, pp. 1544–1551, 2010.

[19] R. D. Cramer, P. Cruz, G. Stahl et al., "Virtual screening for R-groups, including predicted pIC50 contributions, within large structural databases, using Topomer CoMFA," *Journal of Chemical Information and Modeling*, vol. 48, no. 11, pp. 2180–2195, 2008.

[20] R. D. Cramer, "Topomer CoMFA: a design methodology for rapid lead optimization," *Journal of Medicinal Chemistry*, vol. 46, no. 3, pp. 374–388, 2003.

[21] R. J. Jilek and R. D. Cramer, "Topomers: a validated protocol for their self-consistent generation," *Journal of Chemical Information and Computer Sciences*, vol. 44, no. 4, pp. 1221–1227, 2004.

[22] R. D. Cramer, D. E. Patterson, and J. D. Bunce, "Comparative molecular field analysis (CoMFA). 1: effect of shape on binding of steroids to carrier proteins," *Journal of the American Chemical Society*, vol. 110, no. 18, pp. 5959–5967, 1988.

[23] S. Rännar, F. Lindgren, P. Geladi, and S. Wold, "A PLS kernel algorithm for data sets with many variables and fewer objects—part 1: theory and algorithm," *Journal of Chemometrics*, vol. 8, no. 2, pp. 111–125, 1994.

[24] A. Cherkasov, E. N. Muratov, D. Fourches et al., "QSAR modeling: where have you been? Where are you going to?" *Journal of Medicinal Chemistry*, vol. 57, no. 12, pp. 4977–5010, 2014.

[25] R. D. Cramer, "The inevitable QSAR renaissance," *Journal of Computer-Aided Molecular Design*, vol. 26, no. 1, pp. 35–38, 2012.

[26] M. Böhm, J. Stürzebecher, and G. Klebe, "Three-dimensional quantitative structure–activity relationship analyses using comparative molecular field analysis and comparative molecular similarity indices analysis to elucidate selectivity differences of inhibitors binding to trypsin, thrombin, and factor Xa," *Journal of Medicinal Chemistry*, vol. 42, no. 3, pp. 458–477, 1999.

[27] J. Verma, V. Khedkar, and E. Coutinho, "3D-QSAR in drug design–a review," *Current Topics in Medicinal Chemistry*, vol. 10, no. 1, pp. 95–115, 2010.

[28] M. T. Cronin and T. W. Schultz, "Pitfalls in QSAR," *Journal of Molecular Structure: THEOCHEM*, vol. 622, no. 1-2, pp. 39–51, 2003.

[29] S. Marquina, M. Maldonado-Santiago, J. N. Sánchez-Carranza et al., "Design, synthesis and QSAR study of 2′-hydroxy-4′-alkoxy chalcone derivatives that exert cytotoxic activity by the mitochondrial apoptotic pathway," *Bioorganic & Medicinal Chemistry*, vol. 27, no. 1, pp. 43–54, 2019.